Modal analysis of self-aligning ball bearing using finite element method

Navdeep Minhas*, S. S. Banwait

Department of Mechanical Engineering, NITTTR, Chandigarh, Chandigarh, India

Presented in International Conference on Advancements and Futuristic Trends in Mechanical and Materials Engineering held at Indian Institute of Technology Ropar (IITR), Rupnagar, during December 5-7, 2019.

ABSTRACT

The present work consist of vibration analysis of self-aligning ball bearing using simulation. The structural analysis of bearing help us to predict service life. The incipient defects are hard to predict and analyze. The time domain and frequency domain analysis were two major area's used to predict the defects in the bearings. In the present work, the finite element model of the bearing SKF 1205 EKTN9 was created using commercial modeling software and further, analyzed with ANSYS Workbench for the acceleration in Y-direction and results were compared with the standard analytical method.

KEYWORDS

Finite Element Model,
Vibration Analysis,
Transient Structural Analysis.

1. Introduction

The rotor-bearing systems have been of interest to researchers for many decades. Appropriate selection of a bearing type for a given application plays an important role in avoiding early fatigue failure and thereby ensures finite bearing life. The study of its vibrational characteristics must be done to avoid any failure before the life span [1]. The bearing type used in the present work is a double row self-aligning ball bearing. They are the most popular of all rolling bearing because it is non-separable, capable of operating at moderate speeds and require little maintenance in service. In addition, they have a price advantage. The bearing model 1205 EKTN9 from SKF have been used in the study. This bearing has a tapered bore diameter of 25 mm with taper off 1:12 and widely used for many applications [2]. Experimental vibration analysis, structural dynamics and finite element analysis are used to study and analyze the dynamic properties of the structure. Mostly noise, vibration or breakdown issues in mechanical structures arise by the intense dynamic action of the structure.

*Corresponding author,
E-mail: navdeep.mech17@nitttrchd.ac.in

The common occurrence of defects like cracks and pits are located at the inner race, rolling element and outer race [3]. The series of impacts and impulses were generated every time the ball rolls over the defect due to metallic contacts. The energy of each impulse was extended over a broad range of frequencies. Thus, due to the low energy obtained over a spectrum, it is arduous to determine the fault frequency [4]. Therefore, it can easily be masked by low energy noise and frequencies.

Further researchers developed various techniques like time and frequency domain analysis to overcome this problem [5]. The various statistical parameters were used in the time domain analysis to evaluate the default frequencies like kurtosis, root means square (R.S.M), peak values, crest factors, etc [6]. But researchers have encountered problems in evaluating the defect frequencies in the frequency domain for incipient defects [7], Many propound methods have been developed for the bearing faults evaluation such as spectral entropy, wavelet transformation, envelope spectrum, etc [8]. Since it is difficult to detect the vibration signal for incipient defects many of the researchers have proposed a new method like digital twin method to evaluate the vibration signature of the incipient defect [9].

The present work is focused on the idea of simulation of ball bearing fault at the outer race. The transient structural analysis of the ball bearing at different speeds was done. The nodal acceleration in Y-direction was obtained with respect to time. Further, For the simulation results and the analytical calculations the time interval between the impacts was compared. It was observed that the simulated ball pass frequency for outer race matches the analytical approach with some negligible error. Researchers have simulated the more accurate model of full bearings assembly [10].

2. Bearing Defects and Fundamental Fault Frequencies

A common type of defects occuring in the ball bearing are the cracks and pits. generally, they occur at the outer race and inner race, sometimes on the rolling element of the bearing itself. the rotating balls roll over the defect during operation and generates the series of impulses which are categorized into four different fundamental fault frequencies of the bearing [12].

1. Inner raceway ball pass frequency (BPFI) = The angular velocity of the inner raceway relative to cage and the rate at which a fixed point on the cage passes over a fixed point on the ring.
2. Outer raceway ball pass frequency (BPFO) =The angular velocity of the outer ring relative to cage and the rate at which a fixed point on the cage passes over a fixed point on the ring.
3. Fundamental train frequency (FTF) = The angular velocity of the cage over a fixed point.
4. Ball Spin frequency (BSF) = The rotation of the rolling element about own axis.

The frequencies mentioned above are the function of the bearing geometry. These fundamental fault frequencies can be calculated using the following equations:

$$BPFI = \frac{N}{2} \times F \times \left(1 + \frac{B}{d_m} Cos(\theta)\right) \quad (1)$$

$$BPFO = \frac{N}{2} \times F \times \left(1 - \frac{B}{d_m} Cos(\theta)\right) \quad (2)$$

$$FTF = \frac{F}{2} \times \left(1 - \frac{B}{d_m} Cos(\theta)\right) \quad (3)$$

$$BSF = \frac{d_m}{2B} \times F \times \left(1 - \left[\frac{B}{d_m} Cos(\theta)\right]^2\right) \quad (4)$$

where

N = Number of rolling elements in the single raceway,

d_b= Ball element diameter,

d_p= Pitch diameter of the ball bearing,

θ = Bearing contact angle,

F = Shaft frequency/rotating speed.

Vibration Generation Due to Defects in a Ball Bearing

As the ball rolls over the defect, the series of the impact of high energy damped oscillations were generated. The impact was periodic in nature due to the cage presence. Cage is used to as a separator to aviod the mutual contact of the rolling elements.

For the incipient defects, the damped oscillations were masked by the low energy oscillation over the frequency domain so it is challenging to pinpoint the defect frequency and system noise. The rig shown in figure 1 consists of SKF 1205 EKTN9 subjected to tests was used to acquire the data and the high energy impacts are clearly identifiable (shown in fig.2) in the time domain analysis as high energy exponentially decay oscillations due to there periodic nature when compared to the frequency domain. The impulses

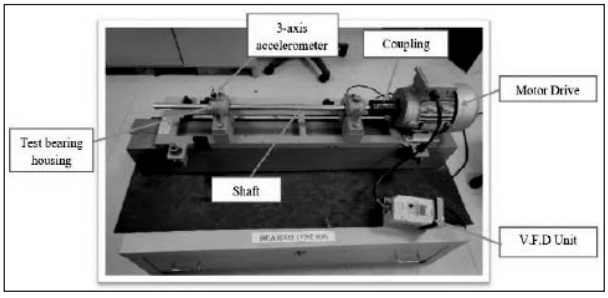

Fig. 1. Experimental setup.

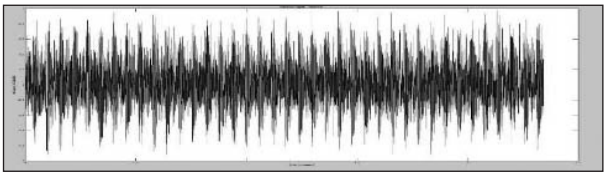

Fig. 2. Vibration signature of the faulty bearing at 1000 rpm under no-load condition.

are very short in time so it is difficult to analyze it in the frequency domain.

Load Distribution

The load in the bearing is generally supported by the rolling elements and transmitted through one raceway to the other raceway. The relationship between the load (Q) and deformation (δ) is following equation (5).

$$Q = k\,\delta^{n} \qquad (5)$$

where Q = load, k = load-defelection factor, δ = deformation and n = 1.5 for ball bearing and n = 1.11 for roller bearing.

Transient Structural Analysis

In the transient structural analysis, the dynamic behavior of the structure were analyzed under the applied boundary condition. Non-linear effects of mass, stiffness, damping, and inertia were considered for the solution. The governing equation for the transient structural analysis used is given below.

$$[M]\{\ddot{x}\} + [C]\{\dot{x}\} + [k]\{x\} = \{F\} \qquad (6)$$

where [M] = mass matrix, [C] = damping matrix, [k] = stiffness matrix and {F} = external force, {x} = displacement vector and {ẋ} = velocity vector and {ẍ} = acceleration vector.

Simulation of Bearing Fault

The SKF 1205 EKTN9 self-aligning bearing was used in this study is shown in figure 3 and its dimensions are given in Table 1. A CAD model of the bearing was created using geometric modeling software Solid Works as shown in figure 4.

For the Finite element analysis, the ANSYS workbench was used and to reduce the simulation non-linearities and computational

Table 1
Dimensions.

S.NO.	Dimensions	Value
1	N	13
2	d_b	7.5mm
3	θ	10.583°
4	d_p	38.376mm

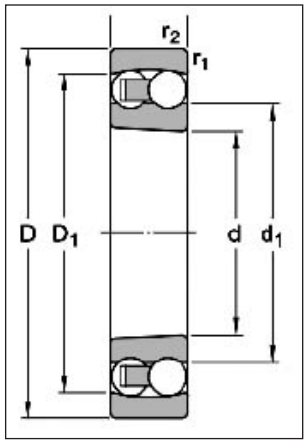

Fig. 3. Self-Aligning ball bearing geometry.

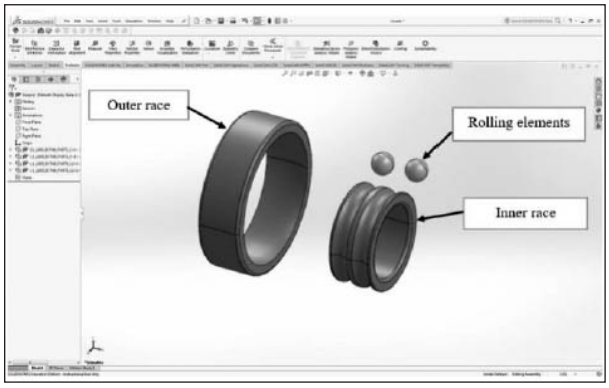

Fig. 4. CAD model view.

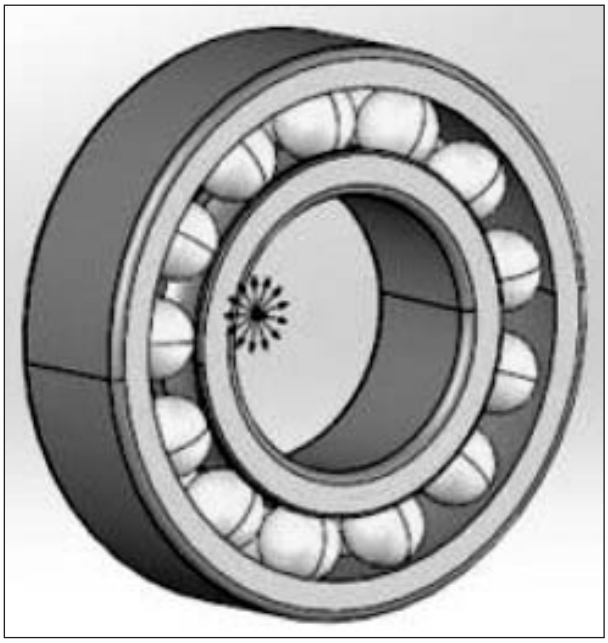

Fig. 5. Assembled CAD model view.

time, only single rolling element shown in figure 6 was considered over the raceways. No cage was considered. As it does not have much effect over the behavior of the dynamic forces in the

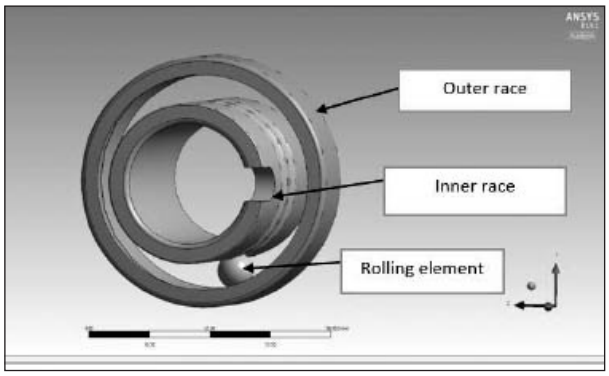

Fig. 6. Healthy bearing in ANSYS workbench.

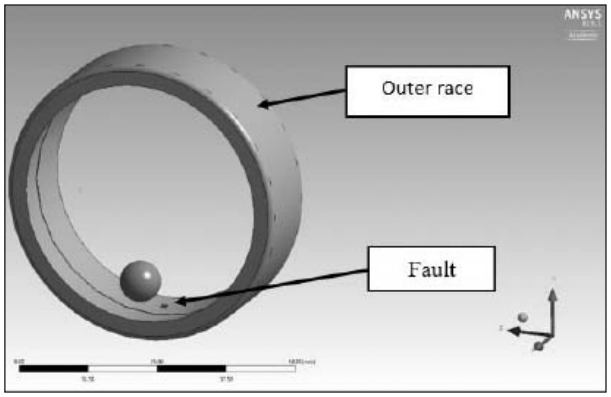

Fig. 7. Outer race with defect.

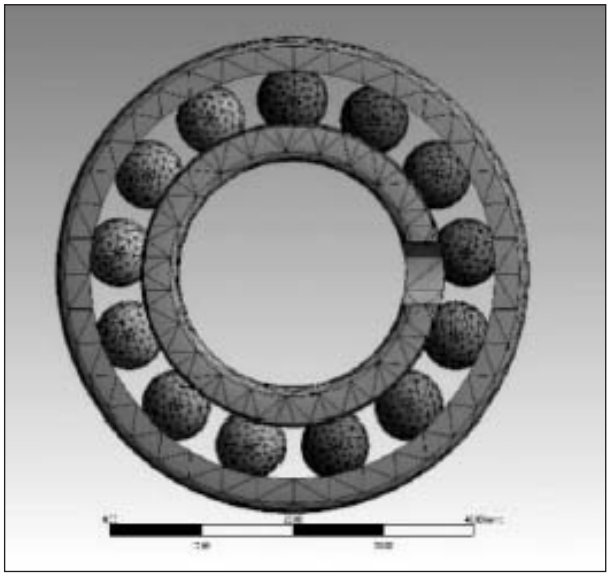

Fig. 8. After meshing.

bearing [11]. The size of defect 1.2mm x 1.2mm was generated over the outer raceway of the bearing as shown in figure 7.

The effects on the outer raceway were counted for this simulation. The dynamic response of the node 1515 and 678 were analyzed. The material

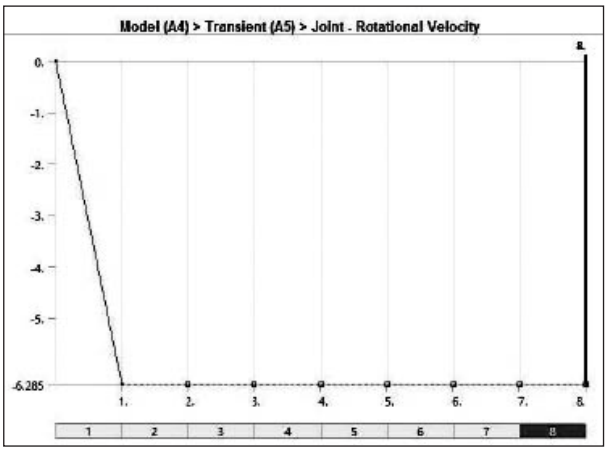

Fig. 9. Rotational velocity applied to the ball bearing in the ansys.

Table 2
Properties of materials used for ball bearing analysis.

Materials	Young's Modulus, E (GPa)	Poisson's Ratio, μ	Density, ρ(kg/m^3)
Steel 100cr6 (raceway material)	210 GPa	0.30	7.81 g/cm^3
Silicon nitride (rolling element)	305 GPa	0.23	3.21 g/cm^3

properties used for the bearing are given below in Table 2.

The metal to metal contact between the raceway and rolling element was considered to be frictional with a frictional coefficient of μ = 0.2. The model of bearing was discretized with body element tetrahedron as shown in figure 8.

Application of Boundary Conditions

The transient structural analysis was carried out on the ANSYS workbench. The outer race was considered as fixed support and the rotational velocity of 60 and 40 RPM were given to the inner race. Simulation for both rotational velocities was carried out and increase in Y-directional acceleration and stresses were observed.

The rotational velocity was incremented in the first step to 60 and 40 RPM and then the inner race was made to run for the time period of 8 seconds to generate adequate results as shown in the figure 9.

3. Results and Discussion

The bearing pass frequency is assoiciated with the defects. When rolling element passes over the defect it generates a impulse of high amplitude. The time interval between the impacts can be calculated analytically or can be observed experimentally. In this work the idea to simulate the time interval between impacts for the different angular velocities is executed.

The solution for the bearing pass frequency for the outer race was obtained analytically and with simulation. The vibration response of the node 1515 and 678 was obtained on the ANSYS workbench. The Y-direction acceleration response was obtained for the thirteenth strike of the same rolling element. The time between the impacts was calculated analytically and with simulation.

Analytical Approach

Both these frequencies are the functions of the number of balls, shaft rotational frequency. The outer race ball pass frequency was determined by equation (1) as mentioned above.

Outer raceway ball pass frequency (BPFO) for 60 RPM = 5.251 Hz.

Outer raceway ball pass frequency (BPFO) for 40 RPM = 3.500 Hz.

Time period for consecutive impacts for 60 RPM = 0.190439916s.

Time period for consecutive impacts for 40 RPM = 0.285714286s.

Therefore, the time period for the same rolling element hits the fault to generate the impact for the 60 and 40 RPM comes out to be 2.47571891s and 3.71428572s.

Simulated Approach

The analysis was carried out on the workbench and acceleration results were obtained. The damped oscillation impacts were noticed between the equal time intervals. similar effects have been noticed by other researchers [12].

The two geometries (healthy and faulty) of the bearing from the modeling software were imported to the ANSYS workbench for the simulation at two different angular velocities. Firstly, the two geometries made to run at 60 RPM and the result for the acceleration signature, frictional stress and von-mises stress was obtained and compared. Similar procedure was adopted for the 40 RPM. When the ball bearing element passes over the defects it generated the high frequency oscillations as shown in the figure 10 for 60 RPM and similarly in figure 11 for 40 RPM.

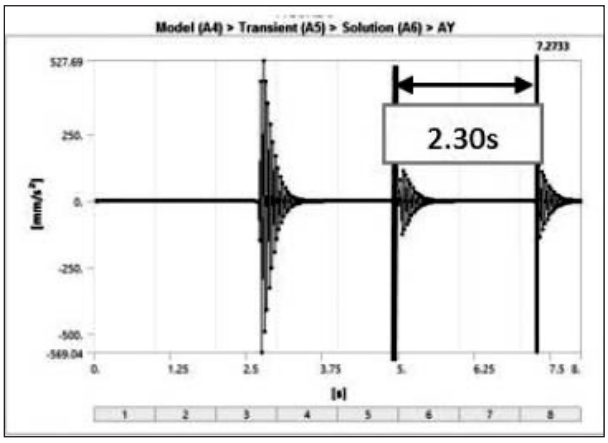

Fig. 10. The Acceleration vs Time plot for the defective bearing (outer race) 60 RPM.

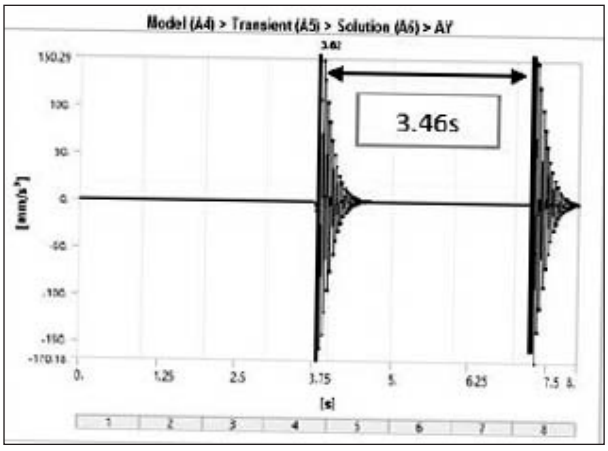

Fig. 11. The Acceleration Vs Time plot for the defective bearing (outer race) 40 RPM.

The acceleration signal was analyzed in the time domain and it shows that there are impulse signal at regular periods that consist of damped oscillations of high-frequency as shown in figure 10. and figure 11., resembling consequences were reported by the researcher's studies. The figure 10 shows the time interval between the stricks over the defect and the acceleration it generates at 60 RPM. Similarly figure 11 shows the results for 40 RPM. The reciprocal of the time difference between two consecutive impulses were noted and this was refered as BPFO.

Table 3
Comparison between analytical and simulated solution.

S. No.	RPM	Bearing Pass Frequency of Outer Race Results		% Error
		Analytical	Simulation	
1	60	2.4761s	2.30s	4.95%
2	40	3.714s	3.46s	6.83%

Table 4
Y-Direction acceleration for faulty and healthy bearing.

S. NO.	RPM	Vibration Response for Healthy Bearing	Vibration Response for Faulty (Outer race) Bearing	% Increase
1	60	-71.84 mm/s^2	-123.73 mm/s^2	72.23%
2	40	-43.758 mm/s^2	-108.07 mm/s^2	146.97%

Table 5
The stresses response for the healthy and faulty bearing.

	Healthy bearing (60 RPM)	Healthy bearing (40 RPM)	Faulty bearing (outer race at 60 RPM)	Faulty bearing (outer race at 40 RPM)
Frictional stress (MPa)	332.92	215.48	654.83	344.75
Principal von-mises stress (MPa)	940.41	688.3	2827.6	2292.9

In table 3, the time interval obtained by simulation and calculated analytically were compared.

The solution (Table 4) in terms of Y-component of acceleration was obtained. The acceleration response for the healthy and bearing with defect at 60 and 40 RPM were compared. These reponses were obtained at the node id 1515 for 60 RPM and 678 for 40 RPM On the ANSYS workbench.

Similarly, the results for the stresses shown in the table 5 were obtained at same node id's on the ANSYS workbench. The increase in the stresses over the faulty area was obtained.

4. Conclusion

The increase in the acceleration and stress concentration proves the validity of the conducted simulation. The error between the mathematically calculated bearing pass frequency for the outer race and the simulated outer race frequency is 4.95% for 60 RPM and 6.83% for the 40 RPM which is less the 10% acceptable error. Therefore, the conducted simulation was found feasible for the selected RPM's.

The increase in the stresses on the faulty bearing signifies the presence of defect on the raceway.

References

1. Ghalamchi, B., Sopance, J., & Mikkola, A. (2013). Simple Versatile Dynamic Model of Spherical Roller Bearing. *International Journal of Rotating Machinery*. 2013. 1-3.
2. SKF catalog, Rolling Bearing (2018).
3. Norton, M. P., (1989). *Fundamentals of Noise and Vibration Analysis for Engineers* (1st ed.). Cambridge University Press. 518–554.
4. Tandon, N., & Choudhury, A. (1999). A review of vibration and acoustic measurement methods for the detection of defects in rolling element bearings. *Tribology International*. 32(8), 469–480.
5. Piñeyro, J., Klempnow, A., & Lescano, V. (2000). Effectiveness of new spectral tools in the anomaly detection of rolling element bearings. *Journal of Alloys and Compounds*. 310 (1-2), 276–279.
6. Goreczk, S., & Strackeljan, J. (2009, June 23-25). *Optimization of time domain features for rolling bearing fault diagnostics.* In The

6th International Conference on Condition Monitoring and Machinery Failure Prevention Technologies, Dublin, Ireland, 42–652.

7. Su, Y.-T., & Sheen, Y.-T. (1993). On the Detectability of Roller Bearing Damage by Frequency Analysis. *Proceedings of the Institution of Mechanical Engineers, Part C: Journal of Mechanical Engineering Science*. 207(1), 23–32.
8. Jiang, R., Chen, J., Dong, G., Liu, T., & Xiao, W. (2012). The weak fault diagnosis and condition monitoring of rolling element bearing using minimum entropy deconvolution and envelop spectrum. *Proceedings of the Institution of Mechanical Engineers, Part C: Journal of Mechanical Engineering Science*. 227(5), 1116–1129.
9. Zahari, T. & Nguyen, T.D. (2010). *Rolling element bearing fault detection with a single point defect on the outer raceway using FEA*. In The 11th Asia Pasific Industrial Engineering & Management Systems Conference.
10. Deshpande, L.G., Sawalhi, N.M., & Randall, R.B. (2012, December 9-12). *Bearing fault simulation using finite element model updating and reduction techniques*. In Proceedings of the 7th Australasian Congress on Applied Mechanics (ACAM 7), Barton, ACT, Australia, 148-154.
11. Lin, T.J., Rong, Q., Li, R.F. & Shao, Y.M. (2009). Finite element analysis for the dynamic characteristic of a deep-groove ball bearing in motion process. *Journal of Vibration and Shock*. 1(1), 28.
12. Tyagi S., & Panigrahi, S. K. (2014). Transient Analysis of Ball Bearing Fault Simulation Using Finite Element Method. *Journal of The Institution of Engineers (India): Series C*. 95(4), 309-318.

Navdeep Minhas Pursuing Ph.D at NIT, Jalandhar. Completed its Masters from NITTTR, Chandigarh. Research interests ranges from tribology, welding and design.

Dr. S. S. Banwait working as Professor at NITTTR, Chandigarh. He obtained his Ph.D from Thaper University in Mechanical Engineering. The researcher interest includes engineering design, production managment, manufacturing technology, non-conventional machining.